Extending the effective-one-body Hamiltonian of black-hole binaries to include next-to-next-to-leading spin-orbit couplings

Enrico Barausse[1] and Alessandra Buonanno[1]

[1]*Maryland Center for Fundamental Physics & Joint Space-Science Institute Department of Physics, University of Maryland, College Park, Maryland 20742, USA*

(Received 14 July 2011; published 11 November 2011)

In the effective-one-body (EOB) approach, the dynamics of two compact objects of masses m_1 and m_2 and spins $\mathbf{S}_1$ and $\mathbf{S}_2$ is mapped into the dynamics of one test particle of mass $\mu = m_1 m_2/(m_1 + m_2)$ and spin $\mathbf{S}_*$ moving in a deformed Kerr metric with mass $M = m_1 + m_2$ and spin $\mathbf{S}_{\rm Kerr}$. In a previous paper, we computed an EOB Hamiltonian for spinning black-hole binaries that (i) when expanded in post-Newtonian orders, reproduces the leading-order spin-spin coupling and the leading and next-to-leading order spin-orbit couplings for any mass ratio, and (iii) reproduces *all* spin-orbit couplings in the test-particle limit. Here we extend this EOB Hamiltonian to include next-to-next-to-leading spin-orbit couplings for any mass ratio. We discuss two classes of EOB Hamiltonians that differ by the way the spin variables are mapped between the effective and real descriptions. We also investigate the main features of the dynamics when the motion is equatorial, such as the existence of the innermost stable circular orbit and of a peak in the orbital frequency during the plunge subsequent to the inspiral.

DOI: 10.1103/PhysRevD.84.104027 PACS numbers: 04.25.D−, 04.25.dg, 04.25.Nx, 04.30.−w

I. INTRODUCTION

Coalescing compact binaries composed of neutron stars and/or black holes are among the most promising gravitational-wave sources for ground-based detectors, such as the Laser Interferometer Gravitational-wave Observatory (LIGO) [1], Virgo [2], GEO [3], the Large Cryogenic Gravitational Telescope [4], and future space-based detectors.

So far, the search for gravitational waves with LIGO, GEO, and Virgo detectors has focused on nonspinning compact binaries [5–9], although in Ref. [10] single-spin templates were used to search for inspiraling spinning compact objects. Within the next 4–5 years, LIGO and Virgo detectors will be upgraded to a sensitivity such that event rates for coalescing binary systems will increase by a factor of 1000. Thus, it is timely and necessary to develop more accurate templates that include spin effects. For maximally spinning objects, we expect that reasonably accurate templates would need to be computed at least through 3.5PN order. In the nonspinning case, studies at the interface between numerical and analytical relativity have demonstrated that templates computed at 3.5PN order are indeed reasonably accurate.

In the last few years, motivated by the search for gravitational waves, the knowledge of spin effects in the two-body dynamics and gravitational-wave emission within the post-Newtonian (PN)[1] approximation has improved considerably. In particular, spin-orbit (SO) effects in the two-body equations of motion are currently known through 3.5PN order (i.e., 2PN order beyond the leading SO term) [11–19], and in the energy flux through 3PN order [12,13,20–23] (i.e., 1.5PN order beyond the leading SO term). Moreover, spin-spin (SS) effects have been computed through 3PN order (i.e., 1PN order beyond the leading SS term) in the conservative dynamics [11,20,24–34] and also in the multipole moments [35].

In order to build reliable templates and search for gravitational-waves from high-mass compact binaries that merge in the detector bandwidth, it is crucial to improve the PN approximation by resumming the dynamics and gravitational emission in a suitable way and by using numerical relativity and perturbation theory as a guidance. The effective-one-body approach (EOB) [36–40] offers the possibility of fulfilling this goal. The EOB approach uses the results of PN theory, not in their original Taylor-expanded form (i.e., as polynomials in v/c), but instead in a suitably resummed form. In particular, it maps the dynamics of two compact objects of masses m_1 and m_2, and spins $\boldsymbol{S}_1$ and $\boldsymbol{S}_2$, into the dynamics of one test particle of mass $\mu = m_1 m_2/(m_1 + m_2)$ and spin $\boldsymbol{S}_*$ moving in a deformed Kerr metric with mass $M = m_1 + m_2$ and spin $\boldsymbol{S}_{\rm Kerr}$. The deformation parameter is the symmetric mass ratio $\eta = m_1 m_2/(m_1 + m_2)^2$, which ranges between 0 (test-particle limit) and $1/4$ (equal-mass limit). The analyses and theoretical progress made in Refs. [41–57] have demonstrated that faithful EOB templates describing the full signal (i.e., the inspiral, merger and ringdown) can be built and used in real searches [9].

Here we build on previous work [39,46,58,59], employ the recent results of Ref. [19], and extend the EOB conservative dynamics, i.e. the EOB Hamiltonian, through 3.5PN order in the SO couplings. Since the mapping between the PN-expanded Hamiltonian (or real Hamiltonian) and the EOB Hamiltonian is not unique, we explore two

[1]We refer to n PN as the order equivalent to terms $O(c^{-2n})$ in the equations of motion beyond the Newtonian acceleration.

specific classes of EOB Hamiltonians, which differ by the way the spin variables of the real and effective descriptions are mapped.

This paper is organized as follows. In Sec. II, after reviewing the logic underpinning the construction of the EOB Hamiltonian, we proceed in steps and extend the EOB Hamiltonian proposed in Ref. [46] through 3.5PN order in the SO couplings. In particular, in Sec. II A we derive the PN-expanded Arnowitt-Deser-Misner (ADM) Hamiltonian in the EOB canonical coordinates; then, after computing in Sec. II B the effective Hamiltonian corresponding to the canonically transformed PN-expanded ADM Hamiltonian, we compare it (in Sec. II C) to the deformed Kerr Hamiltonian for a spinning test particle [46], and work out (in Secs. II D and II E) two classes of EOB Hamiltonians. In Sec. III, we study the dynamics of these Hamiltonians for equatorial orbits, and in Sec. IV we summarize our main conclusions.

We use geometric units $G = c = 1$ throughout the paper, except when performing PN expansions, where powers of the speed of light c are restored and play the role of book-keeping parameters.

II. THE EFFECTIVE-ONE-BODY HAMILTONIAN FOR TWO SPINNING BLACK HOLES

The main ingredient of the EOB approach is the *real* PN-expanded ADM Hamiltonian (or real Hamiltonian) describing two black holes with masses m_1, m_2 and spins $\boldsymbol{S}_1$, $\boldsymbol{S}_2$. The real Hamiltonian is then canonically transformed and subsequently *mapped* to an *effective* Hamiltonian $H_{\rm eff}$ describing a test particle of mass $\mu = m_1 m_2/(m_1 + m_2)$ and suitable spin $\boldsymbol{S}^*$, moving in a *deformed* Kerr metric of mass $M = m_1 + m_2$ and suitable spin $\boldsymbol{S}_{\rm Kerr}$. The deformation is regulated by the binary's symmetric mass-ratio parameter, $\eta = \mu/M$, and therefore disappears in the test-particle limit $\eta \to 0$. The so-called improved real (or EOB) Hamiltonian reads

$$H_{\rm real}^{\rm improved} = M\sqrt{1 + 2\eta\left(\frac{H_{\rm eff}}{\mu} - 1\right)}. \tag{1}$$

The computation of the EOB Hamiltonian consists of several steps. We briefly review these steps and the underlying logic that we will follow in the next sections:

(i) We apply a canonical transformation to the PN-expanded ADM Hamiltonian using the Lie method, obtaining the PN-expanded Hamiltonian in EOB canonical coordinates (see Sec. II A);
(ii) We compute the effective Hamiltonian corresponding to the canonically transformed PN-expanded ADM Hamiltonian (see Sec. II B);
(iii) We PN-expand the deformed-Kerr Hamiltonian for a spinning test-particle derived in Ref. [46] (see Sec. II C);
(iv) We compare (ii) and (iii), and work out the mapping between the spin variables in the real and effective descriptions, and compute the improved EOB Hamiltonian (see Secs. II D and II E).

A. The ADM Hamiltonian canonically transformed to EOB coordinates

Following Ref. [46], we denote the ADM canonical variables in the binary's center-of-mass frame with $\boldsymbol{r}'$ and $\boldsymbol{p}'$, and we introduce the following spin variables:

$$\boldsymbol{\sigma} = \boldsymbol{S}_1 + \boldsymbol{S}_2, \tag{2}$$

$$\boldsymbol{\sigma}^* = \boldsymbol{S}_1\frac{m_2}{m_1} + \boldsymbol{S}_2\frac{m_1}{m_2}. \tag{3}$$

Henceforth, to keep track of the PN orders, we rescale the spins variables as $\boldsymbol{\sigma}^* \to \boldsymbol{\sigma}^* c$ and $\boldsymbol{\sigma} \to \boldsymbol{\sigma} c$.

We use the spin-independent part of the ADM Hamiltonian through 3PN order [38], and we include SO effects through 2PN order beyond the leading-order effects (1.5PN), thus through 3.5PN order. In particular, the ADM SO Hamiltonian at 3.5PN order was computed recently in Ref. [19] (the ADM SO Hamiltonian at 1.5PN was computed in Ref. [60], and at 2.5PN in Ref. [58]). In the binary's center-of-mass, the ADM SO Hamiltonian reads

$$H_{\rm SO}^{\rm ADM}(\boldsymbol{r}', \boldsymbol{p}', \boldsymbol{\sigma}^*, \boldsymbol{\sigma}) = \frac{1}{c^3}\frac{\boldsymbol{L}'}{r'^3}\cdot(g_{\sigma}^{\rm ADM}\boldsymbol{\sigma} + g_{\sigma^*}^{\rm ADM}\boldsymbol{\sigma}^*), \tag{4}$$

where we indicate $\boldsymbol{L}' = \boldsymbol{r}' \times \boldsymbol{p}'$ and

$$g_{\sigma}^{\rm ADM} = 2 + \frac{1}{c^2}\left[\frac{19}{8}\eta\hat{\boldsymbol{p}}'^2 + \frac{3}{2}\eta(\boldsymbol{n}'\cdot\hat{\boldsymbol{p}}')^2 - (6 + 2\eta)\frac{M}{r'}\right] + \frac{1}{c^4}\left[\frac{15}{16}\eta^2(\boldsymbol{n}'\cdot\hat{\boldsymbol{p}}')^4 + \frac{21}{2}(1+\eta)\left(\frac{M}{r'}\right)^2 + \frac{1}{8}\eta(-9 + 22\eta)\hat{\boldsymbol{p}}'^4 - \frac{1}{16}\eta(314 + 39\eta)\frac{M}{r'}\hat{\boldsymbol{p}}'^2 - \frac{1}{16}\eta(256 + 45\eta)\frac{M}{r'}(\boldsymbol{n}'\cdot\hat{\boldsymbol{p}}')^2 + \frac{3}{16}\eta(-4 + 9\eta)\hat{\boldsymbol{p}}'^2(\boldsymbol{n}'\cdot\hat{\boldsymbol{p}}')^2\right], \tag{5a}$$

$$g_{\sigma^*}^{\rm ADM} = \frac{3}{2} + \frac{1}{c^2}\left[\left(-\frac{5}{8} + 2\eta\right)\hat{\boldsymbol{p}}'^2 + \frac{3}{4}\eta(\boldsymbol{n}'\cdot\hat{\boldsymbol{p}}')^2 - (5 + 2\eta)\frac{M}{r'}\right] + \frac{1}{c^4}\left[\frac{1}{8}(75 + 82\eta)\left(\frac{M}{r'}\right)^2 + \frac{1}{16}(7 - 37\eta + 39\eta^2)\hat{\boldsymbol{p}}'^4 - \frac{3}{16}(-18 + 86\eta + 13\eta^2)\frac{M}{r'}\hat{\boldsymbol{p}}'^2 - \frac{3}{16}\eta(32 + 15\eta)\frac{M}{r'}(\boldsymbol{n}'\cdot\hat{\boldsymbol{p}}')^2 + \frac{9}{16}\eta(-1 + 2\eta)\hat{\boldsymbol{p}}'^2(\boldsymbol{n}'\cdot\hat{\boldsymbol{p}}')^2\right], \tag{5b}$$

with $\boldsymbol{n}' = \boldsymbol{r}'/r'$, and where we have introduced the rescaled conjugate momentum $\hat{\boldsymbol{p}}' = \boldsymbol{p}'/\mu$.

In order to canonically transform the ADM Hamiltonian to EOB coordinates, various approaches are possible. A popular method, used in the previous work on the EOB model [37,38,58], is to use a generating function that produces a near-identity transformation, i.e. one of the form $\tilde{G}(q', \pi) = q'^i \pi_i + \epsilon G(q', \pi)$, where (q, π) are the phase variables (including the angles defining the spins and their conjugate momenta; see Ref. [59]) and ϵ is a small parameter. Expressing the initial "primed" coordinates (the ADM coordinates) in terms of the new "unprimed" coordinates (the EOB coordinates), one gets

$$q'^i = q^i - \epsilon \frac{\partial G(q', \pi)}{\partial \pi_i} = q^i - \epsilon \frac{\partial G(q, \pi)}{\partial \pi_i} + \epsilon^2 \frac{\partial^2 G(q, \pi)}{\partial \pi_i \partial q^j} \frac{\partial G(q, \pi)}{\partial \pi_j} + \mathcal{O}(\epsilon^3), \tag{6a}$$

$$\pi'_i = \pi_i + \epsilon \frac{\partial G(q', \pi)}{\partial q'^i} = \pi_i + \epsilon \frac{\partial G(q, \pi)}{\partial q^i} - \epsilon^2 \frac{\partial^2 G(q, \pi)}{\partial q^i \partial q^j} \frac{\partial G(q, \pi)}{\partial \pi_j} + \mathcal{O}(\epsilon^3). \tag{6b}$$

Because under a time-independent canonical transformation the Hamiltonian transforms as $H(q, p) = H'(q', p')$, Eqs. (6) imply

$$\begin{aligned} H(q, \pi) &= H'(q', \pi') \\ &= H'(q, \pi) + \epsilon \left[\frac{\partial H'(q, \pi)}{\partial \pi_i} \frac{\partial G(q, \pi)}{\partial q^i} - \frac{\partial H'(q, \pi)}{\partial q^i} \frac{\partial G(q, \pi)}{\partial \pi_i} \right] + \epsilon^2 \left[\frac{\partial H'(q, \pi)}{\partial q^i} \frac{\partial^2 G(q, \pi)}{\partial \pi_i \partial q^j} \frac{\partial G(q, \pi)}{\partial \pi_j} \right. \\ &\quad - \frac{\partial H'(q, \pi)}{\partial \pi_i} \frac{\partial^2 G(q, \pi)}{\partial q^i \partial q^j} \frac{\partial G(q, \pi)}{\partial \pi_j} + \frac{1}{2} \frac{\partial^2 H'(q, \pi)}{\partial q^i \partial q^j} \frac{\partial G(q, \pi)}{\partial \pi_i} \frac{\partial G(q, \pi)}{\partial \pi_j} + \frac{1}{2} \frac{\partial^2 H'(q, \pi)}{\partial \pi_i \partial \pi_j} \frac{\partial G(q, \pi)}{\partial q^i} \frac{\partial G(q, \pi)}{\partial q^j} \\ &\quad \left. - \frac{\partial^2 H'(q, \pi)}{\partial q^i \partial \pi_j} \frac{\partial G(q, \pi)}{\partial \pi_i} \frac{\partial G(q, \pi)}{\partial q^j} \right] + \mathcal{O}(\epsilon^3). \end{aligned} \tag{7}$$

The terms of order $\mathcal{O}(\epsilon)$ in this equation can be rewritten as $\epsilon\{G, H'\}$, which is very convenient because it transforms a sum over all the phase variables (including the angles defining the spins and their conjugate momenta) into a Poisson bracket that can be computed using only the commutation relations $\{x^i, p_j\} = \delta^i_j$, $\{x^i, S^j_{(a)}\} = 0$, $\{p_i, S^j_{(a)}\} = 0$, and $\{S^i_{(a)}, S^j_{(b)}\} = \delta_{(a)(b)} \epsilon_{ijk} S^k_{(a)}$ ($a, b = 1, 2$ being indices that distinguish between the two black holes). Unfortunately, the terms $\mathcal{O}(\epsilon^2)$ cannot be easily expressed in terms of Poisson brackets, which makes them hard to compute (because the spin variables must be carefully taken into account in the sums). Also, the generalization of Eq. (7) to higher orders in ϵ becomes more and more complicated.

A possible alternative to the generating function method mentioned above is given by the so-called Lie method [61]. This approach exploits the fact that the flux of the Hamilton equations is canonical. Therefore, one can define a fictitious Hamiltonian $\mathcal{H}(q, \pi)$ whose flux sends some initial data (q, π) to $(q'(q, \pi, \epsilon), \pi'(q, \pi, \epsilon))$, where ϵ is the "time" variable of this fictitious Hamiltonian. The canonical transformation is then simply given by $(q'(q, \pi, \epsilon), \pi'(q, \pi, \epsilon))$. The advantage of this approach is that any function $f(q, \pi)$ satisfies $\dot{f} = \{f, \mathcal{H}\}$ (where we denote with $\dot{} = d/d\epsilon$) under the Hamiltonian flux of $\mathcal{H}$. Defining for convenience $\mathcal{G} = -\mathcal{H}$, this equation becomes $\dot{f} = \{\mathcal{G}, f\}$, and denoting the differential operator $\{\mathcal{G}, \ldots\}$ by $\mathcal{L}_{\mathcal{G}}$, a Taylor expansion yields

$$\begin{aligned} f(q'(q, \pi, \epsilon), \pi'(q, \pi, \epsilon)) &= \sum_{n=0}^{\infty} \frac{\epsilon^n}{n!} \mathcal{L}^n_{\mathcal{G}} f(q, \pi) \\ &= \exp(\epsilon \mathcal{L}_{\mathcal{G}}) f(q, \pi) \\ &= f(q, \pi) + \epsilon \{\mathcal{G}, f\}(q, \pi) \\ &\quad + \frac{1}{2} \epsilon^2 \{\mathcal{G}, \{\mathcal{G}, f\}\}(q, \pi) + \mathcal{O}(\epsilon^3). \end{aligned} \tag{8}$$

Specializing to the (nonfictitious) Hamiltonian H', we obtain the equivalent of Eq. (7), that is

$$\begin{aligned} H(q, \pi) &= H'(q', \pi') \\ &= H'(q, \pi) + \epsilon \{\mathcal{G}, H'\}(q, \pi) \\ &\quad + \frac{1}{2} \epsilon^2 \{\mathcal{G}, \{\mathcal{G}, H'\}\}(q, \pi) + \mathcal{O}(\epsilon^3). \end{aligned} \tag{9}$$

As already mentioned, the above expression allows us to account for the spin variables very easily, if necessary,[2] by means of the commutation relations $\{x^i, S^j_{(a)}\} = 0$, $\{p_i, S^j_{(a)}\} = 0$, and $\{S^i_{(a)}, S^j_{(b)}\} = \delta_{(a)(b)} \epsilon_{ijk} S^k_{(a)}$.

In this paper we will use the Lie method to generate the canonical transformation from ADM to EOB coordinates. In particular, we assume

[2]The Poisson brackets of the spin variables with themselves do not enter in the computations that we perform in this paper, but they do enter at higher PN orders.

$$\mathcal{G}(\boldsymbol{r},\boldsymbol{p}) = \boldsymbol{r}\cdot\boldsymbol{p} + \mathcal{G}_{\rm NS}(\boldsymbol{r},\boldsymbol{p}) + \mathcal{G}_{\rm S}(\boldsymbol{r},\boldsymbol{p},\boldsymbol{\sigma}^*,\boldsymbol{\sigma}), \quad (10)$$

where $\mathcal{G}_{\rm NS}$ is the purely orbital part of the fictitious Hamiltonian, while $\mathcal{G}_{\rm S}$ is the spin-dependent part, which we assume to be linear in the spins since in this paper we focus on the SO terms only. Because the transformations (7) and (9) agree at leading order in the perturbative parameter ϵ, G and $\mathcal{G}$ must agree at leading PN order. In particular, since the purely orbital generating function for the transformation from ADM to EOB coordinates starts at 1PN, $\mathcal{G}_{\rm NS}$ must start at 1PN order too, that is

$$\mathcal{G}_{\rm NS}(\boldsymbol{r},\boldsymbol{p}) = \mathcal{G}_{\rm NS1PN}(\boldsymbol{r},\boldsymbol{p}) + \mathcal{G}_{\rm NS2PN}(\boldsymbol{r},\boldsymbol{p}) + \mathcal{O}\left(\frac{1}{c^6}\right), \quad (11)$$

where $\mathcal{G}_{\rm NS1PN}$ must coincide with $G_{\rm NS1PN}$, and therefore be given by [37]

$$\mathcal{G}_{\rm NS1PN}(\boldsymbol{r},\boldsymbol{p}) = \frac{1}{c^2}(\boldsymbol{r}\cdot\boldsymbol{p})\left[-\frac{1}{2}\eta\hat{\boldsymbol{p}}^2 + \frac{M}{r}\left(1+\frac{1}{2}\eta\right)\right]. \quad (12)$$

At 2PN, instead, $\mathcal{G}_{\rm NS}$ does not coincide with $G_{\rm NS}$, but a computation similar to the one in Ref. [37] easily shows that

$$\mathcal{G}_{\rm NS2PN}(\boldsymbol{r},\boldsymbol{p}) = \frac{1}{c^4}(\boldsymbol{r}\cdot\boldsymbol{p})\left[\alpha\hat{\boldsymbol{p}}^4 + \beta\frac{M}{r}\hat{\boldsymbol{p}}^2 + \gamma\frac{M}{r}(\boldsymbol{n}\cdot\hat{\boldsymbol{p}})^2 + \delta\left(\frac{M}{r}\right)^2\right], \quad (13)$$

with

$$\alpha = \frac{\eta}{8}, \qquad \beta = \frac{\eta}{4}(4-\eta), \quad (14a)$$

$$\gamma = \eta\frac{4+\eta}{8}, \qquad \delta = \frac{1-7\eta+\eta^2}{4}. \quad (14b)$$

[Note that the functional form (13) is the same as for $G_{\rm NS2PN}$, but the values of the parameters α, β, γ, and δ are different from those of Ref. [37].]

Similarly, the spin-dependent part of the fictitious Hamiltonian, $\mathcal{G}_{\rm S}$, must start like $G_{\rm S}$ at 2.5PN order:

$$\mathcal{G}_{\rm S}(\boldsymbol{r},\boldsymbol{p},\boldsymbol{\sigma}^*,\boldsymbol{\sigma}) = \mathcal{G}_{\rm S2.5PN}(\boldsymbol{r},\boldsymbol{p},\boldsymbol{\sigma}^*,\boldsymbol{\sigma}) + \mathcal{G}_{\rm S3.5PN}(\boldsymbol{r},\boldsymbol{p},\boldsymbol{\sigma}^*,\boldsymbol{\sigma}) + \mathcal{O}\left(\frac{1}{c^9}\right). \quad (15)$$

and if we restrict to functions that are linear in the spin variables, it must be [15]

$$\mathcal{G}_{\rm S2.5PN}(\boldsymbol{r},\boldsymbol{p},\boldsymbol{\sigma}^*,\boldsymbol{\sigma}) = \frac{1}{c^5 r^3}(\boldsymbol{r}\cdot\hat{\boldsymbol{p}})[a_0(\eta)(\boldsymbol{L}\cdot\boldsymbol{\sigma}) + b_0(\eta)(\boldsymbol{L}\cdot\boldsymbol{\sigma}^*)], \quad (16)$$

where $a_0(\eta)$ and $b_0(\eta)$ are arbitrary gauge functions. [Note that restricting to functions that are linear in the spin variables is justified because here we are looking at SO effects only, but in general cubic terms in the spin may be present; see Ref. [46].]

The most general form for $\mathcal{G}_{\rm S}$ at 3.5PN order is instead, if we restrict again to functions linear in the spins,

$$\mathcal{G}_{\rm S3.5PN}(\boldsymbol{r},\boldsymbol{p}) = \frac{1}{c^7 r^3}(\boldsymbol{r}\cdot\hat{\boldsymbol{p}})\left\{(\boldsymbol{L}\cdot\boldsymbol{\sigma})\left[a_1(\eta)\hat{\boldsymbol{p}}^2 + a_2(\eta)\frac{M}{r} + a_3(\eta)(\boldsymbol{n}\cdot\hat{\boldsymbol{p}})^2\right] + (\boldsymbol{L}\cdot\boldsymbol{\sigma}^*)[b_1(\eta)\hat{\boldsymbol{p}}^2 + b_2(\eta)\frac{M}{r} + b_3(\eta)(\boldsymbol{n}\cdot\hat{\boldsymbol{p}})^2]\right\}, \quad (17)$$

where $a_i(\eta)$ and $b_i(\eta)$ with $i = 1, 2, 3$ are other arbitrary gauge functions. To ease the notation, henceforth we drop the η dependence in the gauge parameters, both at 2.5PN and 3.5PN order, and will denote them simply with a_i and b_i (with $i = 0, 3$).

Applying Eq. (9), we obtain that the 3.5 SO Hamiltonian in EOB coordinates is given by

$$\begin{aligned} H_{\rm SO3.5PN} = {} & H^{\rm ADM}_{\rm SO3.5PN} + \{\mathcal{G}_{\rm NS2PN}, H^{\rm ADM}_{\rm SO1.5PN}\} \\ & + \{\mathcal{G}_{\rm NS1PN}, H^{\rm ADM}_{\rm SO2.5PN}\} + \{\mathcal{G}_{\rm S2.5PN}, H^{\rm ADM}_{\rm 1PN}\} \\ & + \{\mathcal{G}_{\rm S3.5PN}, H^{\rm ADM}_{\rm Newt}\} + \frac{1}{2}\{\mathcal{G}_{\rm NS1PN}, \{\mathcal{G}_{\rm NS1PN}, H^{\rm ADM}_{\rm SO1.5PN}\}\} \\ & + \frac{1}{2}\{\mathcal{G}_{\rm NS1PN}, \{\mathcal{G}_{\rm S2.5PN}, H^{\rm ADM}_{\rm Newt}\}\} \\ & + \frac{1}{2}\{\mathcal{G}_{\rm S2.5PN}, \{\mathcal{G}_{\rm NS1PN}, H^{\rm ADM}_{\rm Newt}\}\}. \end{aligned} \quad (18)$$

A tedious but straightforward calculation gives the several terms entering the above equation:

$$\{\mathcal{G}_{\rm NS2PN}, H^{\rm ADM}_{\rm SO1.5PN}\} = \frac{3}{c^7 r^3}\boldsymbol{L}\cdot\left(2\boldsymbol{\sigma} + \frac{3}{2}\boldsymbol{\sigma}^*\right)\left[\delta\left(\frac{M}{r}\right)^2 + \alpha\hat{\boldsymbol{p}}^4 + \beta\frac{M}{r}\hat{\boldsymbol{p}}^2 + 4\alpha\hat{\boldsymbol{p}}^2(\boldsymbol{n}\cdot\hat{\boldsymbol{p}})^2 + (2\beta+3\gamma)\frac{M}{r}(\boldsymbol{n}\cdot\hat{\boldsymbol{p}})^2\right], \quad (19)$$

$$\begin{aligned} \{\mathcal{G}_{\rm NS1PN}, H^{\rm ADM}_{\rm SO2.5PN}\} = {} & \frac{1}{c^7 r^3}\boldsymbol{L}\cdot\boldsymbol{\sigma}\left[-4(6+5\eta+\eta^2)\left(\frac{M}{r}\right)^2 - \frac{95}{16}\eta^2\hat{\boldsymbol{p}}^4 + \frac{1}{16}\eta(382+159\eta)\frac{M}{r}\hat{\boldsymbol{p}}^2 - \frac{63}{8}\eta^2\hat{\boldsymbol{p}}^2(\boldsymbol{n}\cdot\hat{\boldsymbol{p}})^2 \right. \\ & \left. - \frac{15}{2}\eta^2(\boldsymbol{n}\cdot\hat{\boldsymbol{p}})^4 + \frac{1}{8}\eta(190+63\eta)\frac{M}{r}(\boldsymbol{n}\cdot\hat{\boldsymbol{p}})^2\right] + \frac{1}{c^7 r^3}\boldsymbol{L}\cdot\boldsymbol{\sigma}^*\left[-2(10+9\eta+2\eta^2)\left(\frac{M}{r}\right)^2 \right. \\ & + \frac{5}{16}\eta(5-16\eta)\hat{\boldsymbol{p}}^4 + \frac{1}{16}(-50+295\eta+144\eta^2)\frac{M}{r}\hat{\boldsymbol{p}}^2 + \frac{3}{8}\eta(5-17\eta)\hat{\boldsymbol{p}}^2(\boldsymbol{n}\cdot\hat{\boldsymbol{p}})^2 \\ & \left. - \frac{15}{4}\eta^2(\boldsymbol{n}\cdot\hat{\boldsymbol{p}})^4 + \frac{1}{8}(10+151\eta+57\eta^2)\frac{M}{r}(\boldsymbol{n}\cdot\hat{\boldsymbol{p}})^2\right], \end{aligned} \quad (20)$$

$$\{\mathcal{G}_{\rm S2.5PN}, H^{\rm ADM}_{\rm 1PN}\} = \frac{1}{c^7 r^3}(a_0 \boldsymbol{L}\cdot\boldsymbol{\sigma} + b_0 \boldsymbol{L}\cdot\boldsymbol{\sigma}^*)\Big[\Big(\frac{M}{r}\Big)^2 + \frac{1}{2}(-1+3\eta)\hat{\boldsymbol{p}}^4 - \frac{3}{2}(3+\eta)\frac{M}{r}\hat{\boldsymbol{p}}^2 + \frac{9}{2}(2+\eta)\frac{M}{r}(\boldsymbol{n}\cdot\hat{\boldsymbol{p}})^2 - \frac{3}{2}(-1+3\eta)\hat{\boldsymbol{p}}^2(\boldsymbol{n}\cdot\hat{\boldsymbol{p}})^2\Big], \tag{21}$$

$$\{\mathcal{G}_{\rm S3.5PN}, H^{\rm ADM}_{\rm Newt}\} = \frac{1}{c^7 r^3}\boldsymbol{L}\cdot\boldsymbol{\sigma}\Big[-a_2\Big(\frac{M}{r}\Big)^2 + a_1\hat{\boldsymbol{p}}^4 + (a_2-a_1)\frac{M}{r}\hat{\boldsymbol{p}}^2 - (4a_2+2a_1+3a_3)\frac{M}{r}(\boldsymbol{n}\cdot\hat{\boldsymbol{p}})^2 - 3(a_1-a_3)\hat{\boldsymbol{p}}^2(\boldsymbol{n}\cdot\hat{\boldsymbol{p}})^2 - 5a_3(\boldsymbol{n}\cdot\hat{\boldsymbol{p}})^4\Big] + \frac{1}{c^7 r^3}\boldsymbol{L}\cdot\boldsymbol{\sigma}^*\Big[-b_2\Big(\frac{M}{r}\Big)^2 + b_1\hat{\boldsymbol{p}}^4 + (b_2-b_1)\frac{M}{r}\hat{\boldsymbol{p}}^2 - (4b_2+2b_1+3b_3)\frac{M}{r}(\boldsymbol{n}\cdot\hat{\boldsymbol{p}})^2 - 3(b_1-b_3)\hat{\boldsymbol{p}}^2(\boldsymbol{n}\cdot\hat{\boldsymbol{p}})^2 - 5b_3(\boldsymbol{n}\cdot\hat{\boldsymbol{p}})^4\Big], \tag{22}$$

$$\{\mathcal{G}_{\rm NS1PN}, \{\mathcal{G}_{\rm NS1PN}, H^{\rm ADM}_{\rm SO1.5PN}\}\} = \frac{3}{4c^7 r^3}\boldsymbol{L}\cdot\Big(2\boldsymbol{\sigma} + \frac{3}{2}\boldsymbol{\sigma}^*\Big)\Big[4(2+\eta)^2\Big(\frac{M}{r}\Big)^2 + 5\eta^2\hat{\boldsymbol{p}}^4 - 9\eta(2+\eta)\frac{M}{r}\hat{\boldsymbol{p}}^2 + 8\eta^2\hat{\boldsymbol{p}}^2(\boldsymbol{n}\cdot\hat{\boldsymbol{p}})^2 - 12\eta(2+\eta)\frac{M}{r}(\boldsymbol{n}\cdot\hat{\boldsymbol{p}})^2 + 20\eta^2(\boldsymbol{n}\cdot\hat{\boldsymbol{p}})^4\Big], \tag{23}$$

$$\{\mathcal{G}_{\rm NS1PN}, \{\mathcal{G}_{\rm S2.5PN}, H^{\rm ADM}_{\rm Newt}\}\} = \frac{1}{c^7 r^3}\boldsymbol{L}\cdot(a_0\boldsymbol{\sigma} + b_0\boldsymbol{\sigma}^*)\Big[-2(2+\eta)\Big(\frac{M}{r}\Big)^2 - \frac{5}{2}\eta\hat{\boldsymbol{p}}^4 + \frac{1}{2}(10+9\eta)\frac{M}{r}\hat{\boldsymbol{p}}^2 - \frac{3}{2}\eta\hat{\boldsymbol{p}}^2(\boldsymbol{n}\cdot\hat{\boldsymbol{p}})^2 - \frac{1}{2}(22+3\eta)\frac{M}{r}(\boldsymbol{n}\cdot\hat{\boldsymbol{p}})^2 + 15\eta(\boldsymbol{n}\cdot\hat{\boldsymbol{p}})^4\Big], \tag{24}$$

$$\{\mathcal{G}_{\rm S2.5PN}, \{\mathcal{G}_{\rm NS1PN}, H^{\rm ADM}_{\rm Newt}\}\} = \frac{1}{c^7 r^3}\boldsymbol{L}\cdot(a_0\boldsymbol{\sigma} + b_0\boldsymbol{\sigma}^*)\Big[-(2+\eta)\Big(\frac{M}{r}\Big)^2 - 2\eta\hat{\boldsymbol{p}}^4 + 3(1+\eta)\frac{M}{r}\hat{\boldsymbol{p}}^2 + 6\eta\hat{\boldsymbol{p}}^2(\boldsymbol{n}\cdot\hat{\boldsymbol{p}})^2 - \frac{3}{2}(2+5\eta)\frac{M}{r}(\boldsymbol{n}\cdot\hat{\boldsymbol{p}})^2\Big]. \tag{25}$$

Also, we have [46]

$$H_{\rm Newt} = H^{\rm ADM}_{\rm Newt}, \tag{26a}$$

$$H_{\rm 1PN} = H^{\rm ADM}_{\rm 1PN} + \{\mathcal{G}_{\rm NS1PN}, H^{\rm ADM}_{\rm Newt}\}, \tag{26b}$$

$$H_{\rm SO1.5PN} = H^{\rm ADM}_{\rm SO1.5PN}, \tag{26c}$$

$$H_{\rm SO2.5PN} = H^{\rm ADM}_{\rm SO2.5PN} + \{\mathcal{G}_{\rm S2.5PN}, H^{\rm ADM}_{\rm Newt}\} + \{\mathcal{G}_{\rm 1PN}, H^{\rm ADM}_{\rm SO1.5PN}\}, \tag{26d}$$

where $H^{\rm ADM}_{\rm Newt}$, $H^{\rm ADM}_{\rm 1PN}$ can be found in Ref. [37], the explicit expressions of $\{\mathcal{G}_{\rm S2.5PN}, H^{\rm ADM}_{\rm Newt}\}$ and $\{\mathcal{G}_{\rm 1PN}, H^{\rm ADM}_{\rm SO1.5PN}\}$ are given in Eqs. (5.20), (5.24) of Ref. [46], while

$$\{\mathcal{G}_{\rm NS1PN}, H^{\rm ADM}_{\rm Newt}\} = \frac{\mu}{c^2}\Big[-\frac{1}{2}(2+\eta)\Big(\frac{M}{r}\Big)^2 - \frac{\eta}{2}\hat{\boldsymbol{p}}^4 + (1+\eta)\frac{M}{r}\hat{\boldsymbol{p}}^2 + \frac{1}{2}(-2+\eta)\frac{M}{r}(\boldsymbol{n}\cdot\hat{\boldsymbol{p}})^2\Big]. \tag{27}$$

Also, we note that Eqs. (26b) and (26d) immediately imply $\mathcal{G}_{\rm 2.5PN} = G_{\rm 2.5PN}$, i.e. the 2.5 PN gauge parameters a_0 and b_0 appearing in Eq. (16) have the same meaning in the Lie method and in the generating function approaches.

B. The spin-orbit terms in the effective Hamiltonian through 3.5PN order

Following Refs. [37,39,62], we map the effective and real two-body Hamiltonians as

$$\frac{H_{\rm eff}}{\mu c^2} = \frac{H^2_{\rm real} - m_1^2 c^4 - m_2^2 c^4}{2m_1 m_2 c^4}, \tag{28}$$

where $H_{\rm real}$ is the real two-body Hamiltonian containing also the rest-mass contribution Mc^2. Expanding Eq. (28) in powers of $1/c$, we have

$$H^{\rm eff}_{\rm SO3.5PN} = H_{\rm SO3.5PN} + \frac{1}{M}(H_{\rm SO1.5PN}H_{\rm 1PN} + H_{\rm SO2.5PN}H_{\rm Newt}). \tag{29}$$

Using Eqs. (18) and (26), we find that through 3.5PN order the SO couplings of the effective Hamiltonian are

$$H^{\rm eff}_{\rm SO} = \frac{1}{c^3}\frac{\boldsymbol{L}}{r^3}\cdot(g^{\rm eff}_{\sigma}\boldsymbol{\sigma} + g^{\rm eff}_{\sigma^*}\boldsymbol{\sigma}^*), \tag{30}$$

where

$$g^{\rm eff}_{\sigma} = 2 + \frac{1}{c^2}\left[\frac{1}{8}(3\eta + 8a_0)\hat{\boldsymbol{p}}^2 - \frac{1}{2}(9\eta + 6a_0)(\boldsymbol{n}\cdot\hat{\boldsymbol{p}})^2 - (\eta + a_0)\frac{M}{r}\right] + \frac{1}{c^4}\left[\frac{1}{2}(-4a_0 - 2a_2 - 18\eta - a_0\eta - 3\eta^2)\left(\frac{M}{r}\right)^2 + \frac{1}{8}(-4a_0 + 8a_1 - 5\eta - 2a_0\eta)\hat{\boldsymbol{p}}^4 + \frac{1}{8}(-4a_0 - 8a_1 + 8a_2 - 34\eta + 6a_0\eta + 11\eta^2)\frac{M}{r}\hat{\boldsymbol{p}}^2 + \frac{3}{16}(8a_0 - 16a_1 + 16a_3 + 12\eta - 20a_0\eta - 13\eta^2)\hat{\boldsymbol{p}}^2(\boldsymbol{n}\cdot\hat{\boldsymbol{p}})^2 + \frac{1}{16}(32a_0 - 32a_1 - 64a_2 - 48a_3 + 140\eta + 48a_0\eta - 3\eta^2)\frac{M}{r}(\boldsymbol{n}\cdot\hat{\boldsymbol{p}})^2 + \frac{5}{16}(-16a_3 + 24a_0\eta + 27\eta^2)(\boldsymbol{n}\cdot\hat{\boldsymbol{p}})^4\right], \tag{31a}$$

$$g^{\rm eff}_{\sigma^*} = \frac{3}{2} + \frac{1}{c^2}\left[\frac{1}{8}(-5 + 4\eta + 8b_0)\hat{\boldsymbol{p}}^2 - \frac{1}{4}(15\eta + 12b_0)(\boldsymbol{n}\cdot\hat{\boldsymbol{p}})^2 - \frac{1}{4}(2 + 5\eta + 4b_0)\frac{M}{r}\right] + \frac{1}{c^4}\left[\frac{1}{8}(-4 - 16b_0 - 8b_2 - 55\eta - 4b_0\eta - 13\eta^2)\left(\frac{M}{r}\right)^2 + \frac{1}{16}(7 - 8b_0 + 16b_1 - 11\eta - 4b_0\eta - \eta^2)\hat{\boldsymbol{p}}^4 + \frac{1}{16}(4 - 8b_0 - 16b_1 + 16b_2 - 59\eta + 12b_0\eta + 24\eta^2)\frac{M}{r}\hat{\boldsymbol{p}}^2 + \frac{3}{16}(8b_0 - 16b_1 + 16b_3 + 19\eta - 20b_0\eta - 14\eta^2)\hat{\boldsymbol{p}}^2(\boldsymbol{n}\cdot\hat{\boldsymbol{p}})^2 + \frac{1}{8}(10 + 16b_0 - 16b_1 - 32b_2 - 24b_3 + 109\eta + 24b_0\eta + 6\eta^2)\frac{M}{r}(\boldsymbol{n}\cdot\hat{\boldsymbol{p}})^2 + \frac{5}{2}(-2b_3 + 3b_0\eta + 3\eta^2)(\boldsymbol{n}\cdot\hat{\boldsymbol{p}})^4\right]. \tag{31b}$$

C. The PN-expanded Hamiltonian of a spinning test-particle in a deformed Kerr spacetime

The deformed Kerr metric was obtained in Ref. [46], and it reads

$$g^{tt} = -\frac{\Lambda_t}{\Delta_t\Sigma}, \tag{32a}$$

$$g^{rr} = \frac{\Delta_r}{\Sigma}, \tag{32b}$$

$$g^{\theta\theta} = \frac{1}{\Sigma}, \tag{32c}$$

$$g^{\phi\phi} = \frac{1}{\Lambda_t}\left(-\frac{\tilde{\omega}^2_{\rm fd}}{\Delta_t\Sigma} + \frac{\Sigma}{\sin^2\theta}\right), \tag{32d}$$

$$g^{t\phi} = -\frac{\tilde{\omega}_{\rm fd}}{\Delta_t\Sigma}. \tag{32e}$$

The potentials in these equations are given by

$$\Delta_t = r^2\left[A(r) + \frac{a^2}{r^2}\right], \tag{33}$$

$$\Delta_r = \Delta_t D^{-1}(r), \tag{34}$$

$$\Lambda_t = (r^2 + a^2)^2 - a^2\Delta_t\sin^2\theta, \tag{35}$$

$$\Sigma = r^2 + a^2\cos\theta^2, \tag{36}$$

and

$$\tilde{\omega}_{\rm fd} = 2aMr + a\eta\omega^0_{\rm fd}M^2 + a\eta\omega^1_{\rm fd}\frac{M^3}{r}, \tag{37}$$

where $\omega^0_{\rm fd}$ and $\omega^1_{\rm fd}$ are two "frame-dragging" parameters (that we will fix later), and where

$$A(r) = 1 - \frac{2M}{r} + \frac{2\eta M^3}{r^3} + \left(\frac{94}{3} - \frac{41}{32}\pi^2\right)\frac{\eta M^4}{r^4}, \tag{38a}$$

$$D^{-1}(r) = 1 + \frac{6\eta M^2}{r^2} + 2(26 - 3\eta)\frac{\eta M^3}{r^3}. \tag{38b}$$

The Hamiltonian of a spinning test particle in the deformed Kerr spacetime is

$$H = H_{\rm NS} + H_{\rm S}, \tag{39}$$

with

$$H_{\rm NS} = \beta^i p_i + \alpha\sqrt{\mu^2 + \gamma^{ij}p_i p_j + \mathcal{Q}_4(p)}, \tag{40}$$

where the term $\mathcal{Q}_4(p)$ is quartic in the space momenta p_i and was introduced in Ref. [62]. Moreover, we have

$$\alpha = \frac{1}{\sqrt{-g^{tt}}}, \tag{41}$$

$$\beta^i = \frac{g^{ti}}{g^{tt}}, \tag{42}$$

$$\gamma^{ij} = g^{ij} - \frac{g^{ti}g^{tj}}{g^{tt}}. \tag{43}$$

and

$$H_{\rm S} = H_{\rm SO} + H_{\rm SS}, \tag{44}$$

where $H_{\rm SO}$ contains the odd terms in the spins (and therefore, in particular, the SO terms) and $H_{\rm SS}$ contains the even terms in the spins (and therefore, in particular, the spin-spin terms of the kind $S_{\rm Kerr}S^*$).

Since here we are interested in the SO couplings, we consider only $H_{\rm SO}$ ($H_{\rm SS}$ can be read from Eq. (4.19) in Ref. [46]):

$$H_{\rm SO} = \frac{e^{2\nu-\tilde{\mu}}(e^{\tilde{\mu}+\nu}-\tilde{B})(\hat{\boldsymbol{p}}\cdot\boldsymbol{\xi}r)(\boldsymbol{S}\cdot\hat{\boldsymbol{S}}_{\rm Kerr})}{\tilde{B}^2\sqrt{Q}\xi^2} + \frac{e^{\nu-2\tilde{\mu}}}{\tilde{B}^2(\sqrt{Q}+1)\sqrt{Q}\xi^2}\{(\boldsymbol{S}\cdot\boldsymbol{\xi})\tilde{J}[\mu_r(\hat{\boldsymbol{p}}\cdot\boldsymbol{v}r)(\sqrt{Q}+1) - \mu_{\cos\theta}(\hat{\boldsymbol{p}}\cdot\boldsymbol{n})\xi^2 - \sqrt{Q}(\nu_r(\hat{\boldsymbol{p}}\cdot\boldsymbol{v}r) + (\mu_{\cos\theta}-\nu_{\cos\theta})(\hat{\boldsymbol{p}}\cdot\boldsymbol{n})\xi^2)]\tilde{B}^2 + e^{\tilde{\mu}+\nu}(\hat{\boldsymbol{p}}\cdot\boldsymbol{\xi}r)(2\sqrt{Q}+1) \times[\tilde{J}\nu_r(\boldsymbol{S}\cdot\boldsymbol{v}) - \nu_{\cos\theta}(\boldsymbol{S}\cdot\boldsymbol{n})\xi^2]\tilde{B} - \tilde{J}\tilde{B}_r e^{\tilde{\mu}+\nu}(\hat{\boldsymbol{p}}\cdot\boldsymbol{\xi}r)(\sqrt{Q}+1)(\boldsymbol{S}\cdot\boldsymbol{v})\}, \tag{45}$$

where $\hat{\boldsymbol{S}}_{\rm Kerr} = \boldsymbol{S}_{\rm Kerr}/S_{\rm Kerr}$, $\boldsymbol{\xi} = \hat{\boldsymbol{S}}_{\rm Kerr}\times\boldsymbol{n}$, $\boldsymbol{v} = \boldsymbol{n}\times\boldsymbol{\xi}$, and where

$$Q = 1 + \frac{\Delta_r(\hat{\boldsymbol{p}}\cdot\boldsymbol{n})^2}{\Sigma} + \frac{(\hat{\boldsymbol{p}}\cdot\boldsymbol{\xi}r)^2\Sigma}{\Lambda_t\sin^2\theta} + \frac{(\hat{\boldsymbol{p}}\cdot\boldsymbol{v}r)^2}{\Sigma\sin^2\theta}, \tag{46}$$

and

$$\nu_r = \frac{r}{\Sigma} + \frac{(r^2+a^2)[(r^2+a^2)\Delta_t' - 4r\Delta_t]}{2\Lambda_t\Delta_t}, \tag{47a}$$

$$\nu_{\cos\theta} = \frac{a^2(r^2+a^2)\cos\theta(r^2+a^2-\Delta_t)}{\Lambda_t\Sigma}, \tag{47b}$$

$$\mu_r = \frac{r}{\Sigma} - \frac{1}{\sqrt{\Delta_r}}, \qquad \mu_{\cos\theta} = \frac{a^2\cos\theta}{\Sigma}, \tag{47c}$$

$$\tilde{B} = \sqrt{\Delta_t}, \qquad \tilde{B}_r = \frac{\sqrt{\Delta_r}\Delta_t' - 2\Delta_t}{2\sqrt{\Delta_r\Delta_t}}, \tag{47d}$$

$$e^{2\tilde{\mu}} = \Sigma, \qquad e^{2\nu} = \frac{\Delta_t\Sigma}{\Lambda_t}, \qquad \tilde{J} = \sqrt{\Delta_r}, \tag{47e}$$

in which we use a prime to denote the derivative with respect to r. To obtain the SO couplings through 3.5PN order, we expand Eq. (39). In particular, it is sufficient to consider the first term in the right-hand side of Eq. (40), and set $a = 0$ (deformed Schwarzschild limit) in Eqs. (45)–(47). Doing so, for the PN-expanded deformed Kerr Hamiltonian we obtain

$$H^{\rm NS}_{\rm SO1.5PN} = \frac{2}{r^3c^3}\boldsymbol{L}\cdot\boldsymbol{S}_{\rm Kerr}, \tag{48a}$$

$$H^{\rm NS}_{\rm SO2.5PN} = \frac{1}{r^3c^5}\eta\omega^0_{\rm fd}\frac{M}{r}\boldsymbol{L}\cdot\boldsymbol{S}_{\rm Kerr}, \tag{48b}$$

$$H^{\rm NS}_{\rm SO3.5PN} = \frac{1}{r^3c^7}\eta\omega^1_{\rm fd}\left(\frac{M}{r}\right)^2\boldsymbol{L}\cdot\boldsymbol{S}_{\rm Kerr}, \tag{48c}$$

and

$$H^{\rm S}_{\rm SO1.5PN} = \frac{3}{2r^3c^3}\boldsymbol{L}\cdot\boldsymbol{S}^*, \tag{49a}$$

$$H^{\rm S}_{\rm SO2.5PN} = \frac{1}{r^3c^5}\boldsymbol{L}\cdot\boldsymbol{S}^*\left[-\frac{1}{2}(1+6\eta)\frac{M}{r} - \frac{5}{8}\hat{\boldsymbol{p}}^2\right], \tag{49b}$$

$$H^{\rm S}_{\rm SO3.5PN} = \frac{1}{r^3c^7}\boldsymbol{L}\cdot\boldsymbol{S}^*\left[\frac{1}{2}(-1-42\eta+6\eta^2)\left(\frac{M}{r}\right)^2 + \frac{7}{16}\hat{\boldsymbol{p}}^4 + \frac{1+6\eta}{4}\left(\frac{M}{r}\right)\hat{\boldsymbol{p}}^2 + \frac{5}{4}\left(\frac{M}{r}\right)(\boldsymbol{n}\cdot\hat{\boldsymbol{p}})^2\right]. \tag{49c}$$

D. The EOB Hamiltonian: spin-mapping dependent on dynamical variables

We now determine the mapping between the spins $\boldsymbol{\sigma}$ and $\boldsymbol{\sigma}^*$ of the effective ADM Hamiltonian and the spins $\boldsymbol{S}_{\rm Kerr}$ and $\boldsymbol{S}^*$ of the EOB Hamiltonian by imposing that the deformed Kerr Hamiltonian given by Eqs. (48) and (49) coincides with the effective Hamiltonian given by Eqs. (30) and (31). As found in Ref. [46], we have to assume that the mapping depends on the orbital dynamical variables $\boldsymbol{p}^2$, $\boldsymbol{n}\cdot\boldsymbol{p}$, and r. The general mapping of the spins has the form

$$\boldsymbol{S}^* = \boldsymbol{\sigma}^* + \frac{1}{c^2}\boldsymbol{\Delta}^{(1)}_{\sigma^*} + \frac{1}{c^4}\boldsymbol{\Delta}^{(2)}_{\sigma^*}, \tag{50a}$$

$$\boldsymbol{S}_{\rm Kerr} = \boldsymbol{\sigma} + \frac{1}{c^2}\boldsymbol{\Delta}^{(1)}_{\sigma} + \frac{1}{c^4}\boldsymbol{\Delta}^{(2)}_{\sigma}. \tag{50b}$$

At 2.5PN order, if we assume $\omega^0_{\rm fd} = 0$ [see Eq. (37)] and $\boldsymbol{\Delta}^{(1)}_{\sigma} = 0$, we have [46]

$$\boldsymbol{\Delta}^{(1)}_{\sigma^*} = \boldsymbol{\sigma}^*\left[\frac{1}{6}(-4b_0+7\eta)\frac{M}{r} + \frac{1}{3}(2b_0+\eta)(Q-1) - \frac{1}{2}(4b_0+5\eta)\frac{\Delta_r}{\Sigma}(\boldsymbol{n}\cdot\hat{\boldsymbol{p}})^2\right] + \boldsymbol{\sigma}\left[-\frac{2}{3}(a_0+\eta)\frac{M}{r} + \frac{1}{12}(8a_0+3\eta)(Q-1) - (2a_0+3\eta)\frac{\Delta_r}{\Sigma}(\boldsymbol{n}\cdot\hat{\boldsymbol{p}})^2\right], \tag{51}$$

and at 3.5PN order, assuming $\omega^1_{\rm fd} = 0$ [see Eq. (37)] and $\boldsymbol{\Delta}^{(2)}_{\sigma} = 0$, we obtain

$$\boldsymbol{\Delta}^{(2)}_{\sigma^*} = \boldsymbol{\sigma}^*\Big[\frac{1}{36}(-56b_0-24b_2+353\eta-60b_0\eta-27\eta^2)\Big(\frac{M}{r}\Big)^2+\frac{5}{3}(-2b_3+3b_0\eta+3\eta^2)\frac{\Delta_r^2}{\Sigma^2}(\boldsymbol{n}\cdot\hat{\boldsymbol{p}})^4$$
$$+\frac{1}{72}(-4b_0+48b_1-23\eta-12b_0\eta-3\eta^2)(Q-1)^2+\frac{1}{36}(-14b_0-24b_1+24b_2-103\eta+66b_0\eta+60\eta^2)\frac{M}{r}(Q-1)$$
$$+\frac{1}{12}(2b_0-24b_1+24b_3+16\eta-30b_0\eta-21\eta^2)\frac{\Delta_r}{\Sigma}(\boldsymbol{n}\cdot\hat{\boldsymbol{p}})^2(Q-1)+\frac{1}{12}(-24b_0-16b_1-32b_2$$
$$-24b_3+47\eta-24b_0\eta-54\eta^2)\frac{M}{r}\frac{\Delta_r}{\Sigma}(\boldsymbol{n}\cdot\hat{\boldsymbol{p}})^2]+\boldsymbol{\sigma}\Big[\frac{1}{9}(-14a_0-6a_2-56\eta-15a_0\eta-21\eta^2)\Big(\frac{M}{r}\Big)^2$$
$$+\frac{5}{24}(-16a_3+24a_0\eta+27\eta^2)\frac{\Delta_r^2}{\Sigma^2}(\boldsymbol{n}\cdot\hat{\boldsymbol{p}})^4+\frac{1}{144}(-8a_0+96a_1-45\eta-24a_0\eta)(Q-1)^2$$
$$+\frac{1}{36}(-14a_0-24a_1+24a_2-109\eta+66a_0\eta+51\eta^2)\frac{M}{r}(Q-1)+\frac{1}{24}(4a_0-48a_1+48a_3+6\eta-60a_0\eta$$
$$-39\eta^2)\frac{\Delta_r}{\Sigma}(\boldsymbol{n}\cdot\hat{\boldsymbol{p}})^2(Q-1)+\frac{1}{24}(-48a_0-32a_1-64a_2-48a_3-16\eta-48a_0\eta-147\eta^2)\frac{M}{r}\frac{\Delta_r}{\Sigma}(\boldsymbol{n}\cdot\hat{\boldsymbol{p}})^2\Big]. \quad (52)$$

Note that as in Ref. [46], we have replaced, in the expressions for $\boldsymbol{\Delta}^{(1)}_{\sigma^*}$ and $\boldsymbol{\Delta}^{(2)}_{\sigma^*}$, the term $\hat{\boldsymbol{p}}^2$ with $\gamma^{ij}\hat{p}_i\hat{p}_j = Q-1$ and the term $(\boldsymbol{n}\cdot\hat{\boldsymbol{p}})^2$ with $\Delta_r(\boldsymbol{n}\cdot\hat{\boldsymbol{p}})^2/\Sigma = g^{rr}\hat{p}_r^2$.

Having determined the spin mappings, we can write down the real improved (or EOB) Hamiltonian for spinning black holes, which turns out to be

$$H^{\rm improved}_{\rm real} = M\sqrt{1+2\eta\Big(\frac{H_{\rm eff}}{\mu}-1\Big)}, \quad (53)$$

where

$$H_{\rm eff} = H_{\rm S}+\beta^i p_i+\alpha\sqrt{\mu^2+\gamma^{ij}p_ip_j+\mathcal{Q}_4(p)}$$
$$-\frac{\mu}{2Mr^3}(\delta^{ij}-3n^in^j)S^*_iS^*_j. \quad (54)$$

E. The EOB Hamiltonian: spin-mapping independent of dynamical variables

In the previous section, we had to assume a dependence on the orbital dynamical variables $\boldsymbol{p}^2$, $\boldsymbol{n}\cdot\boldsymbol{p}$, and r in the mapping between the spins $\boldsymbol{\sigma}$ and $\boldsymbol{\sigma}^*$ of the effective ADM Hamiltonian and the spins $\boldsymbol{S}_{\rm Kerr}$ and $\boldsymbol{S}^*$ of the deformed Kerr Hamiltonian. To avoid this dependence on the dynamical variables and obtain the much simpler mapping

$$\boldsymbol{S}^* = \boldsymbol{\sigma}^*, \quad (55a)$$
$$\boldsymbol{S}_{\rm Kerr} = \boldsymbol{\sigma}, \quad (55b)$$

we need to modify the Hamilton-Jacobi equation by adding terms depending on the momenta and spins. Since in this paper we are dealing only with SO effects, we will neglect modifications that involve spin-spin terms. We start by observing that in the presence of spins the linear momentum P_μ, which is related to the canonical momentum by $P_\mu = p_\mu + E^{\rho\sigma}_\mu S^*_{\rho\sigma}$ [see Eq. (3.28) of Ref. [59]], satisfies the Hamilton-Jacobi equation [59]

$$\mu^2 + P_\mu P^\mu = \mu^2 + p_\mu p^\mu + 2E^{\rho\sigma}_\mu p^\mu S^*_{\rho\sigma} + \mathcal{O}(S^*)^2 = 0. \quad (56)$$

Here, $S^*_{\mu\nu}$ is the spin tensor of the test particle [see Ref. [59] and also Eqs. (2.4)–(2.7) in Ref. [14]]. Equation (56) leads to the correct Hamiltonian for a spinning particle in curved spacetime, at linear order in the particle's spin [59]. To modify the Hamilton-Jacobi equation, a suitable ansatz is

$$\mu^2 + g^{\mu\nu}_{\rm eff}(\mathbf{r},\mathbf{S}_{\rm Kerr})p_\mu p_\nu + 2E^{\rho\sigma}_\mu p^\mu S^*_{\rho\sigma}$$
$$+[B^{\mu\nu\lambda}_{\rho\sigma}(\mathbf{r})p_\mu p_\nu p_\lambda + B^{\mu\nu\lambda\tau\alpha}_{\rho\sigma}(\mathbf{r})p_\mu p_\nu p_\lambda p_\tau p_\alpha]S^{\rho\sigma}_*$$
$$+A^{\mu\nu\lambda\tau}(\mathbf{r},\mathbf{S}_{\rm Kerr})p_\mu p_\nu p_\lambda p_\tau$$
$$+A^{\mu\nu\lambda\tau\rho\sigma}(\mathbf{r},\mathbf{S}_{\rm Kerr})p_\mu p_\nu p_\lambda p_\tau p_\rho p_\sigma+\cdots=0. \quad (57)$$

If we make use at lowest order of the condition $\mu^2 + g^{\mu\nu}_{\rm eff}p_\mu p_\nu \simeq 0$, we can replace p_t with the spatial components of the momentum, and obtain the following generalized form of the effective Hamiltonian

$$H_{\rm eff} = \beta^i p_i + \alpha\sqrt{\mu^2+\gamma^{ij}p_ip_j+\mathcal{Q}_4(p)+\mathcal{Q}_S(r,p,S^*,S_{\rm Kerr})}$$
$$-\frac{\mu}{2Mr^3}(\delta^{ij}-3n^in^j)S^*_iS^*_j+H_{\rm S}, \quad (58)$$

where $\mathcal{Q}_4(p)$ is a quartic term in the momenta [62], which is due to the presence of the quartic term $A^{\mu\nu\lambda\tau}p_\mu p_\nu p_\lambda p_\tau$ in Eq. (57), and $\mathcal{Q}_S(r,p,S^*,S_{\rm Kerr})$ is a term linear in $\boldsymbol{S}_*$ and $\boldsymbol{S}_{\rm Kerr}$

$$\mathcal{Q}_S(r,p,S^*,S_{\rm Kerr}) = \mathcal{Q}^{S_{\rm Kerr}}_i(r,p)S^i_{\rm Kerr}+\mathcal{Q}^{S^*}_i(r,p)S^i_*. \quad (59)$$

In particular, the term $\mathcal{Q}^{S^*}_i(r,p)S^i_*$ comes from the terms $B^{\mu\nu\lambda}_{\rho\sigma}(\mathbf{r})p_\mu p_\nu p_\lambda S^{\rho\sigma}_*$ and $B^{\mu\nu\lambda\tau\alpha}_{\rho\sigma}p_\mu p_\nu p_\lambda p_\tau p_\alpha S^{\rho\sigma}_*$ in Eq. (57), while the term $\mathcal{Q}^{S_{\rm Kerr}}_i(r,p)S^i_{\rm Kerr}$ comes from $A^{t\nu\lambda\tau}p_tp_\nu p_\lambda p_\tau$ and $A^{t\nu\lambda\tau\rho\sigma}p_tp_\nu p_\lambda p_\tau p_\rho p_\sigma$ (through the dependence of the tensors $A^{\mu\nu\lambda\tau}$ and $A^{\mu\nu\lambda\tau\rho\sigma}$ on $\boldsymbol{S}_{\rm Kerr}$). Finally, the term $H_{\rm S}$ in Eq. (58) comes from the presence of $2E^{\rho\sigma}_\mu p^\mu S^*_{\rho\sigma}$ in Eq. (57). As already stressed, this

happens because Eq. (56) leads to the correct Hamiltonian for a spinning particle in curved spacetime, and, in particular, to $H_{\rm S}$, which is the spin-dependent part of that Hamiltonian [59].

Through 3.5PN order the quantities $\mathcal{Q}_i^{S_{\rm Kerr}}(r,p)S^i_{\rm Kerr}$ and $\mathcal{Q}_i^{S^*}(r,p)S^i_*$ must have the form

$$\mathcal{Q}_i^s(r,p)s^i = \frac{\mu}{r^2c^3}\epsilon_{ijk}n^jp^ks^i\times\left\{\frac{1}{c^2}\left(c_1\frac{M}{r}+c_2\hat{\boldsymbol{p}}^2+c_3(\boldsymbol{n}\cdot\hat{\boldsymbol{p}})^2\right)+\frac{1}{c^4}\left[c_4\hat{\boldsymbol{p}}^4+c_5\left(\frac{M}{r}\right)^2+c_6(\boldsymbol{n}\cdot\hat{\boldsymbol{p}})^4+c_7\hat{\boldsymbol{p}}^2\frac{M}{r}+c_8(\boldsymbol{n}\cdot\hat{\boldsymbol{p}})^2\frac{M}{r}+c_9(\boldsymbol{n}\cdot\hat{\boldsymbol{p}})^2\hat{\boldsymbol{p}}^2\right]\right\}, \tag{60}$$

where s stands for either $S_{\rm Kerr}$ or S^*, while the coefficients c_n, $n=1,\ldots 9$ are determined by the mapping of the effective to the real description. A straightforward computation leads to

$$\mathcal{Q}_S = \mathcal{Q}_{S2.5\rm PN} + \mathcal{Q}_{S3.5\rm PN}, \tag{61}$$

where

$$\mathcal{Q}_{S2.5\rm PN}(\mathbf{r},\mathbf{p},\mathbf{S}^*,\mathbf{S}_{\rm Kerr}) = \frac{\mu}{r^3c^5}\left\{(\boldsymbol{S}_{\rm Kerr}\cdot\mathbf{L})\left[-2(a_0+\eta)\frac{M}{r}+\frac{1}{4}(8a_0+3\eta)(Q-1)-3(2a_0+3\eta)\frac{\Delta_r}{\Sigma}(\boldsymbol{n}\cdot\hat{\boldsymbol{p}})^2\right]+(\boldsymbol{S}^*\cdot\mathbf{L})\left[\frac{1}{2}(-4b_0+7\eta)\frac{M}{r}+(2b_0+\eta)(Q-1)-\frac{3}{2}(4b_0+5\eta)\frac{\Delta_r}{\Sigma}(\boldsymbol{n}\cdot\hat{\boldsymbol{p}})^2\right]\right\}, \tag{62}$$

$$\begin{aligned}\mathcal{Q}_{S3.5\rm PN}(\mathbf{r},\mathbf{p},\mathbf{S}^*,\mathbf{S}_{\rm Kerr}) = \frac{\mu}{r^3c^7}\Bigg\{&(\boldsymbol{S}_{\rm Kerr}\cdot\boldsymbol{L})\Bigg[(-6a_0-2a_2-20\eta-a_0\eta-3\eta^2)\left(\frac{M}{r}\right)^2+\frac{5}{8}(-16a_3+24a_0\eta+27\eta^2)\frac{\Delta_r^2}{\Sigma^2}(\boldsymbol{n}\cdot\hat{\boldsymbol{p}})^4\\&+\frac{1}{8}(16a_1-7\eta-4a_0\eta)(Q-1)^2+\frac{1}{4}(-8a_1+8a_2-35\eta+6a_0\eta+11\eta^2)\frac{M}{r}(Q-1)\\&+\frac{3}{8}(-16a_1+16a_3-20a_0\eta-13\eta^2)\frac{\Delta_r}{\Sigma}(\boldsymbol{n}\cdot\hat{\boldsymbol{p}})^2(Q-1)+\frac{1}{8}(-80a_0-32a_1-64a_2-48a_3-64\eta\\&+48a_0\eta-3\eta^2)\frac{M}{r}\frac{\Delta_r}{\Sigma}(\boldsymbol{n}\cdot\hat{\boldsymbol{p}})^2\Bigg]+(\boldsymbol{S}^*\cdot\boldsymbol{L})\Bigg[\frac{1}{4}(-24b_0-8b_2+127\eta-4b_0\eta-37\eta^2)\left(\frac{M}{r}\right)^2\\&+5(-2b_3+3b_0\eta+3\eta^2)\frac{\Delta_r^2}{\Sigma^2}(\boldsymbol{n}\cdot\hat{\boldsymbol{p}})^4+\frac{1}{8}(16b_1-7\eta-4b_0\eta-\eta^2)(Q-1)^2+\frac{1}{8}(-16b_1+16b_2\\&-61\eta+12b_0\eta+24\eta^2)\frac{M}{r}(Q-1)+\frac{3}{8}(-16b_1+16b_3+9\eta-20b_0\eta-14\eta^2)\frac{\Delta_r}{\Sigma}(\boldsymbol{n}\cdot\hat{\boldsymbol{p}})^2(Q-1)\\&+\frac{1}{4}(-40b_0-16b_1-32b_2-24b_3+27\eta+24b_0\eta+6\eta^2)\frac{M}{r}\frac{\Delta_r}{\Sigma}(\boldsymbol{n}\cdot\hat{\boldsymbol{p}})^2\Bigg]\Bigg\}.\end{aligned} \tag{63}$$

Finally, the EOB Hamiltonian is obtained by inserting Eq. (58) into Eq. (53).

III. THE EFFECTIVE-ONE-BODY DYNAMICS FOR EQUATORIAL ORBITS

We stress that the EOB models introduced in the previous sections have the correct test-particle limit, for both nonspinning and spinning black holes (for *generic* orbits and *arbitrary* spin orientations), and that the test-particle limit is recovered nonperturbatively, (i.e., at all PN orders). This is because in order to build our models, in Sec. II C we started from the Hamiltonian derived in Ref. [59], which correctly reproduces the Mathisson-Papapetrou-Pirani equation describing the motion of a classical spinning particle in a generic curved spacetime [63–67]. The EOB models that we present in this paper share this feature with our earlier model [46], which was valid through 3PN order in the nonspinning sector and through 2.5PN order in the spinning sector, but not with other EOB models for spinning black-hole binaries, which recover the test-particle limit only approximately [15].

Other attractive features of our models are evident when considering configurations with spins parallel to the orbital angular momentum, which correspond, in the effective EOB dynamics, to a particle moving on equatorial orbits. For aligned spins and equatorial orbits, in fact, both the models with dynamical and nondynamical spin mapping predict the existence of an innermost stable circular orbits (ISCO), for all values of the system's parameters. This feature is again shared by our earlier model [46], but not by other EOB models for spinning black-hole binaries [15], which do not present ISCOs for large values of the spins. While the nonexistence of an ISCO is not necessarily a sign that a model is flawed, its presence helps reproduce the results of numerical-relativity simulations for binaries with aligned spins [68].

To calculate the radius and the orbital angular momentum at the ISCO for our EOB models, we solve numerically the following system of equations [36]

$$\frac{\partial H^{\rm improved}_{\rm real}(r, p_r = 0, L_z)}{\partial r} = 0, \tag{64}$$

$$\frac{\partial^2 H^{\rm improved}_{\rm real}(r, p_r = 0, L_z)}{\partial r^2} = 0, \tag{65}$$

with respect to r and $L_z = p_\phi$. The solutions can then be used to evaluate the ISCO frequency via

$$\Omega_{\rm ISCO} = \frac{\partial H^{\rm improved}_{\rm real}(r_{\rm ISCO}, p_r = 0, L_z^{\rm ISCO})}{\partial L_z}, \tag{66}$$

which follows immediately from the Hamilton equations.

The values of $r_{\rm ISCO}$ and $L_z^{\rm ISCO}$ can also be used to calculate the binding energy at the ISCO via $E_{\rm bind} = H^{\rm improved}_{\rm real} - M$. This quantity is interesting because it corresponds to the mass lost in gravitational waves during the binary's inspiral, and is therefore a lower limit to the total mass loss, to which it reduces for $\eta \to 0$ (when the fluxes during the merger and the ringdown become negligible [46]). Similarly, one can estimate the spin of the binary at the ISCO via

$$\chi_{\rm ISCO} = \frac{S_1^z + S_2^z + L^z_{\rm ISCO}}{(M + E^{\rm bind}_{\rm ISCO})^2}. \tag{67}$$

This expression clearly neglects the mass and angular momentum lost during the merger and ringdown phases, but it is useful as qualitative diagnostics of our model, and it reduces to the spin of the final black-hole remnant when $\eta \to 0$ (again, because in this limit the fluxes during the merger and the ringdown become negligible [46]).

We rewrite the metric potentials Δ_t and Δ_r given in Eqs. (33) and (34), using the "log-model" of Ref. [46] [see Eqs. (5.71) and (5.73)–(5.83) of that paper], and assume

$$K(\eta) = 1.447 - 0.1574\eta - 9.082\eta^2. \tag{68}$$

The value of $K(\eta)$ for $\eta = 0$ ensures [46,69] that the ISCO frequency for extreme mass-ratio nonspinning binaries predicted by our EOB models agrees with the exact result of Ref. [70], which calculated the shift of the ISCO frequency due to the conservative part of the self-force. The linear and quadratic terms in η in Eq. (68) are such that our EOB models accurately reproduce numerical relativity simulations for nonspinning binaries with mass ratios ranging from $q = 1/6$ to $q = 1$ [68].

We fix the gauge parameters to the following values:

$$a_0 = -\frac{3}{2}\eta, \qquad b_0 = -\frac{5}{4}\eta, \tag{69}$$

$$a_1 = \frac{1}{2}\eta^2, \qquad b_1 = \frac{1}{16}\eta(9 + 5\eta),$$
$$a_2 = \frac{1}{8}\eta(7 - 8\eta), \qquad b_2 = \frac{1}{8}\eta(17 - 5\eta),$$
$$a_3 = -\frac{9}{16}\eta^2, \qquad b_3 = -\frac{3}{8}\eta^2, \tag{70}$$

which we determine by requiring that all the terms involving $\Delta_r \hat{\boldsymbol{p}} \cdot \boldsymbol{n}/\Sigma$ cancel out in $\boldsymbol{\Delta}^{(1)}_{\sigma^*}$ and $\boldsymbol{\Delta}^{(2)}_{\sigma^*}$ [Eqs. (51) and (52)], or equivalently in $\mathcal{Q}_{S2.5\rm PN}$ and $\mathcal{Q}_{S3.5\rm PN}$ [Eqs. (62) and (63)]. Different choices of the gauge parameters produce qualitatively similar results for the ISCO quantities that we described above.

Focusing on systems with spins aligned with the orbital angular momentum $\boldsymbol{L}$, and denoting with $S_{1,2} = \chi_{1,2} m_{1,2}^2$ the projections of the spins along the direction of $\boldsymbol{L}$, we consider binaries with $\chi_1 = \chi_2 = \chi$ and mass ratios $q = m_2/m_1 = 0.1$, 0.5, and 1. In particular, in Figs. 1–3 we show how the ISCO quantities described above change as a consequence of including the 3.5PN SO terms in our EOB model with dynamical spin mapping. More specifically, we calculate $\Omega_{\rm ISCO} M$, $E^{\rm ISCO}_{\rm bind}/M$, and $\chi_{\rm ISCO}$ using the Hamiltonian (54), with and without the 3.5PN terms given by $\boldsymbol{\Delta}^{(2)}_{\sigma^*}$. As can be seen, the inclusion of the 3.5PN terms does not change the ISCO quantities significantly for $\chi \leq 0$, while small differences appear for $\chi > 0$. (In the case of $\Omega_{\rm ISCO} M$, however, these differences grow quite large when $\chi \to 1$.) Overall, Figs. 1–3 suggest that the model has reasonable convergence properties for radii $r \geq r_{\rm ISCO}$.

The results for the model with nondynamical spin mapping are similar [i.e., a comparison of the ISCO quantities calculated using the Hamiltonian (58), with and without

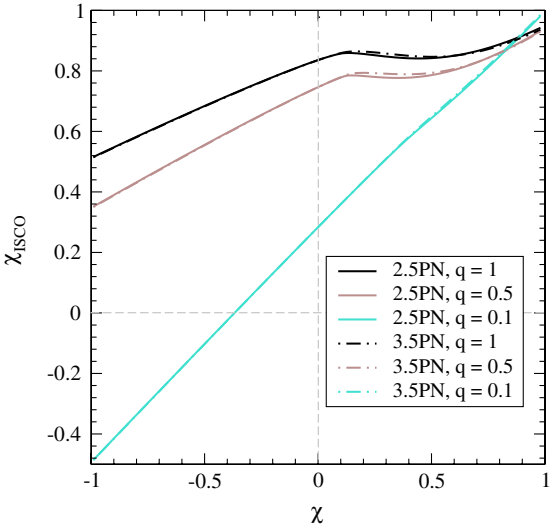

FIG. 1 (color online). The spin parameter of the binary at the ISCO given by Eq. (67) for the 2.5PN and 3.5PN EOB models with dynamical mapping of the spins, for binaries having spins parallel to $\boldsymbol{L}$, mass ratio $q = m_2/m_1$, and spin-parameter projections onto the direction of $\boldsymbol{L}$ given by $\chi_1 = \chi_2 = \chi$.

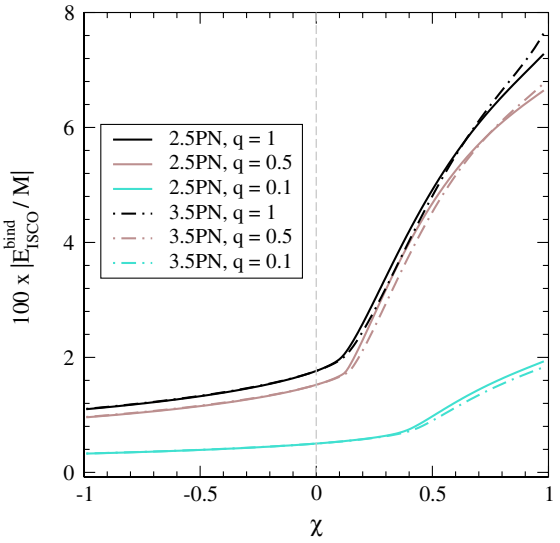

FIG. 2 (color online). The same as in Fig. 1 but for the binding energy of the binary at the ISCO.

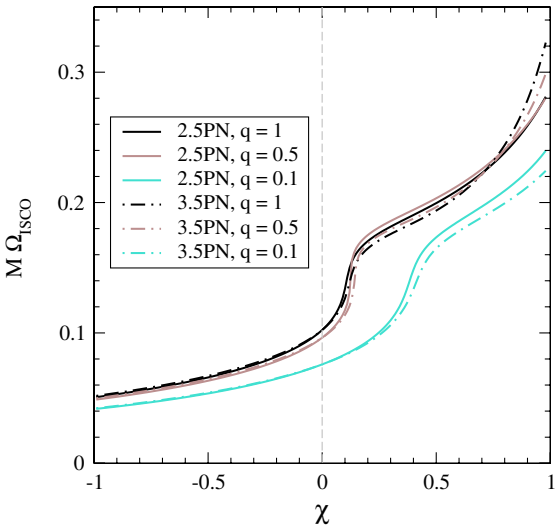

FIG. 3 (color online). The same as in Fig. 1 but for the ISCO frequency.

the 3.5PN term $\mathcal{Q}_{3.5\mathrm{PN}}$, gives similar results]. In general, however, the model with nondynamical spin mapping presents lower values for $\Omega_{\mathrm{ISCO}}M$ at high spins and for comparable mass ratios (see Fig. 4, where we compare the 3.5PN models with dynamical and nondynamical spin mapping).

Another attractive feature of our models is the existence of a peak of the orbital frequency during the plunge starting at the ISCO. More precisely, we assume that the effective particle starts off with no radial velocity at the ISCO (thus having angular momentum L_{ISCO} and energy E_{ISCO}), and we evolve the geodesic equations by calculating the radial momentum p_r during the plunge from energy and angular momentum conservation. We then calculate the orbital

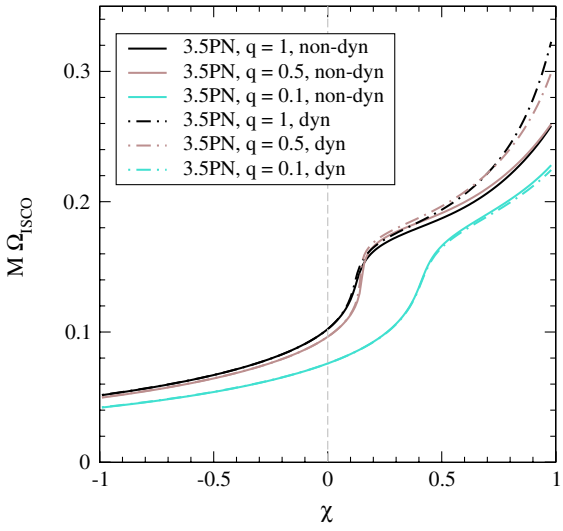

FIG. 4 (color online). The ISCO frequency for the 3.5PN EOB models with dynamical (dyn) and nondynamical (non-dyn) mapping of the spins, for binaries having spins parallel to $\boldsymbol{L}$, mass ratio $q = m_2/m_1$, and spin-parameter projections onto the direction of $\boldsymbol{L}$ given by $\chi_1 = \chi_2 = \chi$.

frequency $\Omega = \partial H^{\mathrm{improved}}_{\mathrm{real}}/\partial L_z$ along the trajectory and find that it presents a peak Ω_{max}. This is not surprising because the same behavior was observed to be generic in our earlier model [46]. The values of $M\Omega_{\mathrm{max}}$ for binaries with spins parallel to $\boldsymbol{L}$, as function of $\chi = \chi_1 = \chi_2$, are shown in Fig. 5 for mass ratios $q = 1$, 0.5, and 0.1, for the EOB model with dynamical spin mapping at 2.5PN and 3.5PN. As can be seen, the differences introduced by the 3.5 PN terms, although reasonable, are larger than for the ISCO quantities. This may be because the plunge happens at radii that are smaller than r_{ISCO} and approach the

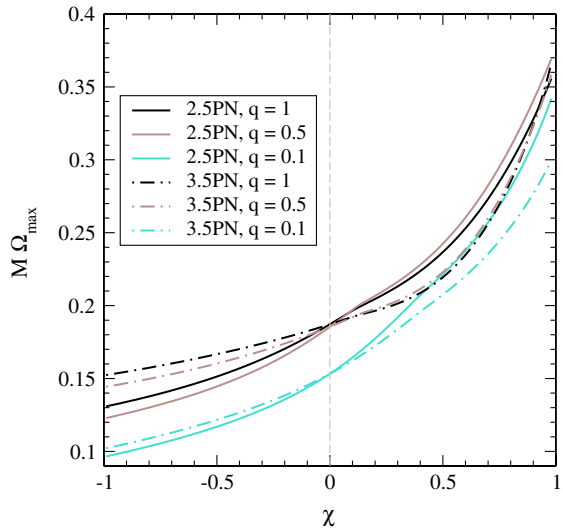

FIG. 5 (color online). The same as in Fig. 1, but for the maximum of the orbital frequency during the plunge.

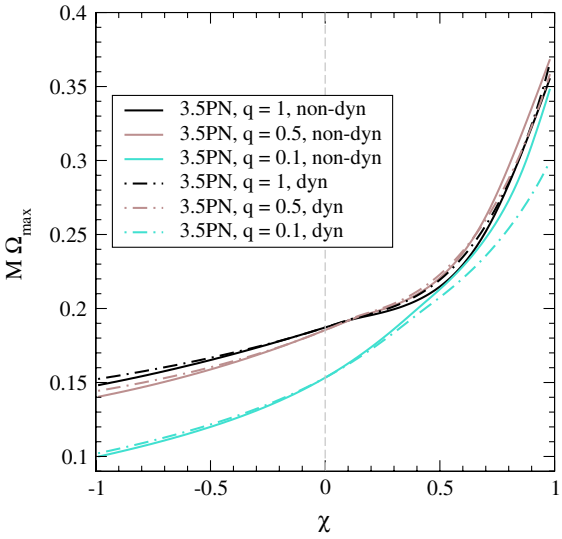

FIG. 6 (color online). The same as in Fig. 4, but for the maximum frequency during the plunge.

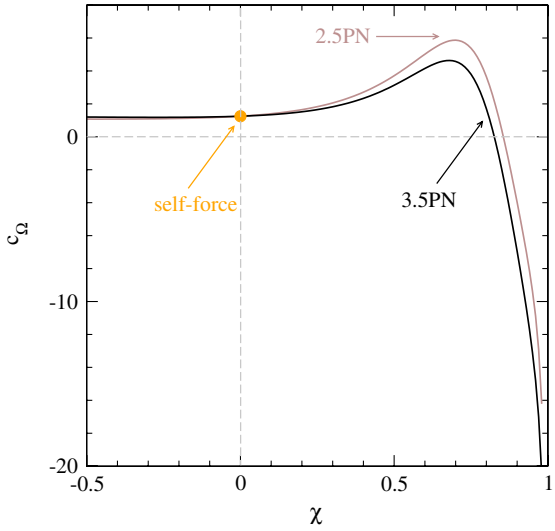

FIG. 7 (color online). The shift of the ISCO frequency c_Ω, defined in Eq. (71), for the 2.5PN and 3.5PN EOB models with dynamical mapping of the spins, for a binary having spins parallel to $\boldsymbol{L}$, mass ratio $q = m_2/m_1 = 10^{-3}$, and spin-parameter projections onto the direction of $\boldsymbol{L}$ given by $\chi_1 = \chi$ and $\chi_2 = 0$.

horizon's radius, thus making the higher-order PN terms more and more important. The results for the model with nondynamical spin mapping are generally similar, although they differ slightly at high spins. In particular, in Fig. 6 we compare the 3.5PN models with dynamical and nondynamical spin mapping. As can be seen, for $q = 0.5$ and $q = 1$ the predictions of the two models are very close, while for $q = 0.1$ the model with dynamical spin mapping presents somewhat lower maximum frequencies.

Also, we stress that the values of $M\Omega_{\rm max}$ for spin antialigned with the angular momentum (i.e., $\chi_1 = \chi_2 = \chi < 0$) are quite sensitive to the values of the gauge parameters a_0–a_3 and b_0–b_3. For instance, setting all the gauge parameters to 0 makes the behavior of $M\Omega_{\rm max}$ with χ nonmonotonic if the 3.5PN models (both with dynamical and nondynamical spin mapping) are considered. This effect does not appear in the 2.5PN models, and can in principle be important for the calibration of our model with numerical-relativity simulations. More details on this will be given in a follow-up paper [68]. Even worse, when the gauge parameters are set to zero, the difference in $M\Omega_{\rm max}$ between the 2.5PN and 3.5PN models is larger than in Fig. 5, a sign that the model probably converges more slowly in this gauge. In light of this, it seems preferable to use the gauge parameters (69) and (70), which by canceling out the radial momentum $\Delta_r \hat{\boldsymbol{p}} \cdot \boldsymbol{n}/\Sigma$ from $\boldsymbol{\Delta}^{(1)}_{\sigma^*}$ and $\boldsymbol{\Delta}^{(2)}_{\sigma^*}$ (and from $\mathcal{Q}_{S2.5\rm PN}$ and $\mathcal{Q}_{S3.5\rm PN}$) provide a rather regular and monotonic behavior for $M\Omega_{\rm max}$ and reasonable differences between the 2.5 and 3.5PN models.

Finally, in Fig. 7 we show the predictions of our EOB model with dynamical spin mapping for the ISCO frequency of a system with $q = m_2/m_1 = 10^{-3}$, $\chi_1 = \chi$, and $\chi_2 = 0$ (the results for the EOB model with nondynamical spin mapping are similar). More precisely, we show the fractional deviation from the Kerr ISCO frequency normalized by the mass ratio,

$$c_\Omega = \frac{1}{q}\left(\frac{\Omega_{\rm ISCO} M|_q}{\Omega_{\rm ISCO} M|_{\rm Kerr}} - 1\right), \tag{71}$$

as a function of χ, as proposed in Ref. [69]. This ISCO shift is caused by the conservative part of the self-force and has been calculated exactly by Ref. [70] in the case of a Schwarzschild spacetime ($\chi = 0$). The results of Ref. [70] is $c_\Omega = 1.2513 + \mathcal{O}(q)$ [see also Ref. [71]], and is denoted by a filled circle in Fig. 7. As can be seen, both the 2.5 and 3.5PN models predict $c_\Omega > 0$, except when $\chi \gtrsim 0.83$. This change of behavior of the EOB prediction is common also to our earlier model of Ref. [46], and might have important implication for configurations that might violate the Cosmic Censorship Conjecture [72,73]. However, the behavior of c_Ω, which seems to diverge as χ approaches 1, suggests that this might simply be a spurious effect due to the incomplete knowledge of the function K [Eq. (68)] and to the fact that the EOB model only reproduces the SS coupling at leading PN order (2PN). As mentioned in Ref. [46], K may in general depend not only on η but also on χ^2, and these spin-dependent terms can be very important for near-extremal spins, and so will the 3PN SS couplings.

It is therefore possible that after reconstructing the full functional form of K (by comparing to future self-force calculations in Kerr or to numerical-relativity simulations for spinning binaries) and extending the EOB model to include the 3PN SS couplings, c_Ω might remain positive even at high spins.

IV. CONCLUSIONS

Recently, Ref. [19] has computed the 3.5PN SO effects in the ADM Hamiltonian. We have taken advantage of this result and extended the EOB Hamiltonian of spinning black holes to include these higher-order SO couplings.

Building on previous work [39,58], and, in particular, on the EOB Hamiltonian of Refs. [46,59], which reproduces the SO test-particle couplings exactly at all PN orders, we have worked out two classes of EOB Hamiltonians, which differ by the way the spin variables are mapped between the effective and real descriptions. One class of EOB Hamiltonians is the straightforward extension to the next PN order of the EOB Hamiltonian of Ref. [46]. It uses a mapping between the real and effective spin variables that depends on the dynamical orbital variables $\mathbf{p}^2, \mathbf{n}\cdot\mathbf{p}$, and r. By contrast, the other class of EOB Hamiltonians uses a mapping between the real and effective spin variables that *does not* depend on these dynamical orbital variables. We achieved this result at the cost of modifying the Hamilton-Jacobi equation of a spinning test particle.

Quite interestingly, when restricting to spins aligned or antialigned with the orbital angular momentum and to equatorial circular orbits, we find that the predictions of these two classes of EOB Hamiltonians for the ISCO frequency, energy and angular momentum, and for the maximum of the orbital frequency during the plunge are generally similar. However, for high spins the model with dynamical mapping of the spins may present somewhat lower maximum frequencies and larger ISCO frequencies.

As pointed out originally in Ref. [58], several gauge parameters can enter the canonical transformation that maps the real and effective Hamiltonians. If the Hamiltonian were known exactly, i.e., at all PN orders, then physical effects should not depend on these parameters. However, since we know the Hamiltonian only at a certain PN order, we expect these gauge parameters to lead to non-negligible differences. In fact, we obtained that when setting all the gauge parameters to zero, the maximum frequency during the plunge has a nonmonotonic dependence on the spins, and varies quite significantly as a consequence of the inclusion of the 3.5 PN SO couplings. We found instead that when choosing the gauge parameters so that the terms depending on the radial momentum disappear from our spin mapping (in the model with dynamical spin mapping) or from the modifications to the Hamilton-Jacobi equation (in the model with nondynamical spin mapping), the maximum frequency during the plunge has a much more regular behavior and varies by small amounts when adding the 3.5PN SO couplings. This suggests that such a choice of the gauge parameters may accelerate the convergence of the model's results in the strong-field region where the plunge takes place.

The EOB Hamiltonians derived in this paper can be calibrated to numerical-relativity simulations with the goal of building analytical templates for LIGO and Virgo searches. A first example was obtained in Ref. [47], where the EOB Hamiltonian at 2.5PN order in the SO couplings of Ref. [58] was calibrated to two highly-accurate numerical simulations. Results that use the EOB Hamiltonian at 3.5PN order developed in this paper will be reported in the near future [68].

Lastly, while finalizing this work, Ref. [74] appeared in the archives as a preprint. Both this paper and Ref. [74] derive the effective gyromagnetic coefficients [see Eq. (31)], but with two different methods. Our computation uses the Lie method to generate both the purely-orbital and the spin-dependent canonical transformations, while Ref. [74] first applies explicitly the purely-orbital transformation from ADM to EOB coordinates, and then uses Eq. (7) to account for the effect of a spin-dependent canonical transformation. As a result of these different procedures, and as discussed in Sec. II A, the 2.5PN gauge parameters in our spin-dependent canonical transformation coincide with those of Ref. [74], but the 3.5PN gauge parameters have different meanings in the two approaches and therefore do not coincide. However, by suitably expressing our 3.5PN gauge parameters in terms of those of Ref. [74], we find that our effective gyromagnetic coefficients fully agree with those of Ref. [74]. This amounts to saying that our gyromagnetic coefficients agree with those of Ref. [74] up to a canonical transformation, and are therefore physically equivalent. More importantly, in this paper we have focused on and worked out two classes of EOB Hamiltonians that are different from the one considered in Ref. [74].

ACKNOWLEDGMENTS

E. B. and A. B. acknowledge support from NSF Grant No. PHY-0903631. A. B. also acknowledges support from NASA Grant No. NNX09AI81G.

[1] B. Abbott *et al.* (LIGO Scientific Collaboration), Rep. Prog. Phys. **72**, 076901 (2009).
[2] F. Acernese *et al.* (Virgo Collaboration), Classical Quantum Gravity **25**, 184001 (2008).
[3] H. Grote (GEO600 Collaboration), Classical Quantum Gravity **25**, 114043 (2008).
[4] K. Kuroda and the LCGT Collaboration, Classical Quantum Gravity **27**, 084004 (2010).

[5] B. Abbott *et al.* (LIGO Scientific Collaboration), Phys. Rev. D **73**, 062001 (2006).
[6] B. Abbott *et al.* (LIGO Scientific Collaboration), Phys. Rev. D **77**, 062002 (2008).
[7] B. P. Abbott *et al.* (LIGO Scientific Collaboration), Phys. Rev. D **80**, 047101 (2009).
[8] J. Abadie *et al.* (LIGO Scientific Collaboration), Phys. Rev. D **82**, 102001 (2010).
[9] J. Abadie *et al.* (LIGO Scientific Collaboration and Virgo), Phys. Rev. D **83**, 122005 (2011).
[10] B. Abbott *et al.* (LIGO Scientific Collaboration), Phys. Rev. D **78**, 042002 (2008).
[11] L. E. Kidder, C. M. Will, and A. G. Wiseman, Phys. Rev. D **47**, 3281 (1993).
[12] B. J. Owen, H. Tagoshi, and A. Ohashi, Phys. Rev. D **57**, 6168 (1998).
[13] H. Tagoshi, A. Ohashi, and B. J. Owen, Phys. Rev. D **63**, 044006 (2001).
[14] G. Faye, L. Blanchet, and A. Buonanno, Phys. Rev. D **74**, 104033 (2006).
[15] T. Damour, P. Jaranowski, and G. Schäfer, Phys. Rev. D **77**, 064032 (2008).
[16] R. A. Porto, Classical Quantum Gravity **27**, 205001 (2010).
[17] D. L. Perrodin, arXiv:1005.0634.
[18] M. Levi, Phys. Rev. D **82**, 104004 (2010).
[19] J. Hartung and J. Steinhoff, Ann. Phys. (N.Y.) **523**, 783 (2011).
[20] L. E. Kidder, Phys. Rev. D **52**, 821 (1995).
[21] C. M. Will, Phys. Rev. D **71**, 084027 (2005).
[22] L. Blanchet, A. Buonanno, and G. Faye, Phys. Rev. D **74**, 104034 (2006).
[23] L. Blanchet, A. Buonanno, and G. Faye, Phys. Rev. D **84**, 064041 (2011).
[24] B. Mikóczi, M. Vasúth, and L. A. Gergely, Phys. Rev. D **71**, 124043 (2005).
[25] R. A. Porto, Phys. Rev. D **73**, 104031 (2006).
[26] R. A. Porto and I. Z. Rothstein, Phys. Rev. Lett. **97**, 021101 (2006).
[27] S. Hergt and G. Schaefer, Phys. Rev. D **77**, 104001 (2008).
[28] J. Steinhoff, S. Hergt, and G. Schaefer, Phys. Rev. D **77**, 081501(R) (2008).
[29] S. Hergt and G. Schäfer, Phys. Rev. D **78**, 124004 (2008).
[30] J. Steinhoff, S. Hergt, and G. Schäfer, Phys. Rev. D **78**, 101503 (2008).
[31] J. Steinhoff, G. Schäfer, and S. Hergt, Phys. Rev. D **77**, 104018 (2008).
[32] R. A. Porto and I. Z. Rothstein, Phys. Rev. D **78**, 044012 (2008).
[33] R. A. Porto and I. Z. Rothstein, Phys. Rev. D **78**, 044013 (2008).
[34] M. Levi, Phys. Rev. D **82**, 064029 (2010).
[35] R. A. Porto, A. Ross, and I. Z. Rothstein, J. High Energy Phys. 03 (2011) 009.
[36] A. Buonanno and T. Damour, Phys. Rev. D **62**, 064015 (2000).
[37] A. Buonanno and T. Damour, Phys. Rev. D **59**, 084006 (1999).
[38] T. Damour, P. Jaranowski, and G. Schäfer, Phys. Rev. D **62**, 084011 (2000).
[39] T. Damour, Phys. Rev. D **64**, 124013 (2001).
[40] A. Buonanno, Y. Chen, and T. Damour, Phys. Rev. D **74**, 104005 (2006).
[41] A. Buonanno, G. B. Cook, and F. Pretorius, Phys. Rev. D **75**, 124018 (2007).
[42] A. Buonanno, Y. Pan, J. G. Baker, J. Centrella, B. J. Kelly, S. T. McWilliams, and J. R. van Meter, Phys. Rev. D **76**, 104049 (2007).
[43] Y. Pan, A. Buonanno, J. G. Baker, J. Centrella, B. J. Kelly, S. T. McWilliams, F. Pretorius, and J. R. van Meter, Phys. Rev. D **77**, 024014 (2008).
[44] M. Boyle, A. Buonanno, L. E. Kidder, A. H. Mroué, Y. Pan, H. P. Pfeiffer, and M. A. Scheel, Phys. Rev. D **78**, 104020 (2008).
[45] A. Buonanno, Y. Pan, H. P. Pfeiffer, M. A. Scheel, L. T. Buchman, and L. E. Kidder, Phys. Rev. D **79**, 124028 (2009).
[46] E. Barausse and A. Buonanno, Phys. Rev. D **81**, 084024 (2010).
[47] Y. Pan, A. Buonanno, L. Buchman, T. Chu, L. Kidder, H. Pfeiffer, and M. Scheel, Phys. Rev. D **81**, 084041 (2010).
[48] Y. Pan, A. Buonanno, R. Fujita, E. Racine, and H. Tagoshi, Phys. Rev. D **83**, 064003 (2011).
[49] T. Damour and A. Nagar, Phys. Rev. D **77**, 024043 (2008).
[50] T. Damour, A. Nagar, E. N. Dorband, D. Pollney, and L. Rezzolla, Phys. Rev. D **77**, 084017 (2008).
[51] T. Damour, A. Nagar, M. Hannam, S. Husa, and B. Brügmann, Phys. Rev. D **78**, 044039 (2008).
[52] T. Damour, B. R. Iyer, and A. Nagar, Phys. Rev. D **79**, 064004 (2009).
[53] T. Damour and A. Nagar, Phys. Rev. D **79**, 081503 (2009).
[54] N. Yunes, A. Buonanno, S. A. Hughes, M. Coleman Miller, and Y. Pan, Phys. Rev. Lett. **104**, 091102 (2010).
[55] N. Yunes *et al.*, Phys. Rev. D **83**, 044044 (2011).
[56] S. Bernuzzi, A. Nagar, and A. Zenginoglu, Phys. Rev. D **83**, 064010 (2011).
[57] Y. Pan, A. Buonanno, M. Boyle, L. T. Buchman, L. E. Kidder *et al.*, arXiv:1106.1021.
[58] T. Damour, P. Jaranowski, and G. Schaefer, Phys. Rev. D **77**, 064032 (2008).
[59] E. Barausse, E. Racine, and A. Buonanno, Phys. Rev. D **80**, 104025 (2009).
[60] T. Damour and G. Schäfer, Nuovo Cimento Soc. Ital. Fis. **101B**, 127 (1988).
[61] G. Benettin, in *Lectures at the Porquerolles School 2001: Hamiltonian Systems and Fourier Analysis*, edited by D. Benest, C. Froeschle, and E. Lega (Cambridge Scientific, Cambridge, England, 2004).
[62] T. Damour, P. Jaranowski, and G. Schäfer, Phys. Rev. D **62**, 084011 (2000).
[63] M. Mathisson, Acta Phys. Pol. **6**, 163 (1937).
[64] A. Papapetrou, Proc. Phys. Soc. London Sect. A **64**, 57 (1951).
[65] A. Papapetrou, Proc. R. Soc. A **209**, 248 (1951).

[66] E. Corinaldesi and A. Papapetrou, Proc. R. Soc. A **209**, 259 (1951).
[67] F. Pirani, Acta Phys. Pol. **15**, 389 (1956).
[68] A. Taracchini *et al.* (unpublished).
[69] M. Favata, Phys. Rev. D **83**, 024028 (2011).
[70] L. Barack and N. Sago, Phys. Rev. Lett. **102**, 191101 (2009).
[71] T. Damour, Phys. Rev. D **81**, 024017 (2010).
[72] E. Barausse, V. Cardoso, and G. Khanna, Phys. Rev. Lett. **105**, 261102 (2010).
[73] E. Barausse, V. Cardoso, and G. Khanna, arXiv:1106.1692.
[74] A. Nagar, arXiv:1106.4349 [Phys. Rev. D (to be published)].